LA-UR-97- -3721

Title: MOLYBDENUM DISILICIDE COMPOSITES PRODUCED BY PLASMA SPRAYING

CONF-980533--

RECEIVED
DEC 16 1997
OSTI

Author(s): RICHARD G. CASTRO, MST-6
KENDALL J. HOLLIS, MST-6
HUIJOU H. KUNG, MST-CMS
ANDREW H. BARTLETT, NORSAM TECHNOLOGY

MASTER

Submitted to: 15TH INTERNATIONAL THERMAL SPRAY CONFERENCE IN NICE, FRANCE ON MAY 25-29, 1998

DISTRIBUTION OF THIS DOCUMENT IS UNLIMITED

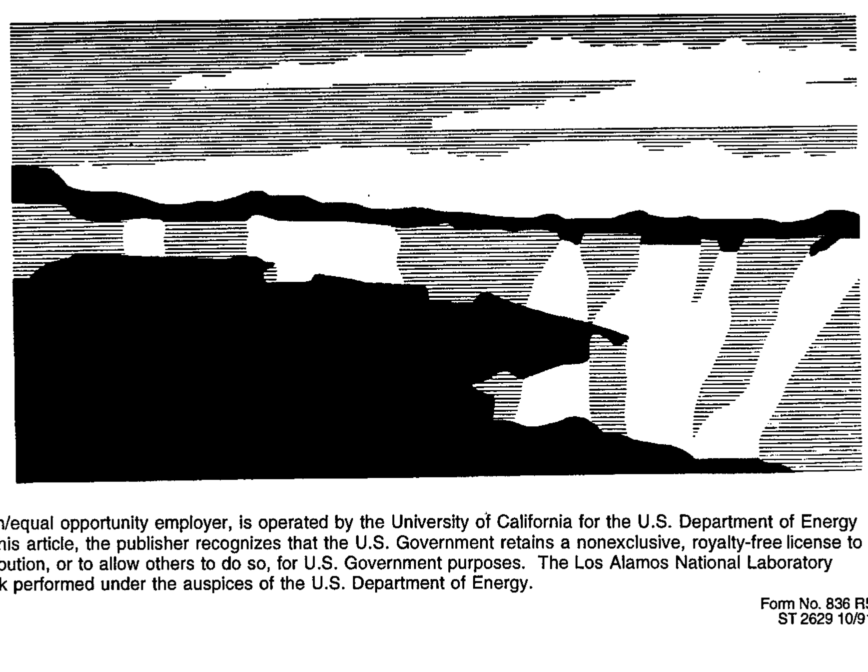

19980420 014

Los Alamos
NATIONAL LABORATORY

DISCLAIMER

Abstract

The intermetallic compound, molybdenum disilicide ($MoSi_2$) is being considered for high temperature structural applications because of its high melting point and superior oxidation resistance at elevated temperatures. The lack of high temperature strength, creep resistance and low temperature ductility has hindered its progress for structural applications. Plasma spraying of coatings and structural components of $MoSi_2$-based composites offers an exciting processing alternative to conventional powder processing methods due to superior flexibility and the ability to tailor properties. Laminate, discontinuous and *in situ* reinforced composites have been produced with secondary reinforcements of Ta, Al_2O_3, SiC, Si_3N_4 and Mo_5Si_3. Laminate composites, in particular, have been shown to improve the damage tolerance of $MoSi_2$ during high temperature melting operations. A review of research which as been performed at Los Alamos National Laboratory on plasma spraying of $MoSi_2$-based composites to improve low temperature fracture toughness, thermal shock resistance, high temperature strength and creep resistance will be discussed.

MOLYBDENUM DISILICIDE ($MoSi_2$) is being considered for high temperature coatings and structural applications in oxidizing and combustion environments. $MoSi_2$ has a number of attractive properties for high temperature applications which includes a melting point of 2030 °C, excellent high temperature oxidation resistance, a brittle-to-ductile transition for polycrystalline $MoSi_2$ of approximately 1000 °C, and thermodynamic stability with a number of ceramic reinforcements (SiC, Si_3N_4, ZrO_2, Al_2O_3, mullite, TiB_2, TiC). $MoSi_2$ is a relatively abundant material which is non-toxic and environmentally benign.

Plasma spraying of $MoSi_2$ has been investigated by a number of researchers as a means of fabricating composite structures containing discontinuous, laminate and reactive sprayed composites (1-9). The advantages of compositing $MoSi_2$ with secondary reinforcements to improve fracture toughness and high temperature strength have been discussed by Petrovic and Vasudevan (10-12). Unlike silicon-based ceramics which sublime upon heating, $MoSi_2$ can be melt processed using plasma spraying and spray-forming techniques. This processing advantage allows the ability to manipulate and tailor the microstructure of $MoSi_2$-based coatings and structural components using secondary reinforcements which are introduced during the deposition process. Incorporating secondary reinforcements in plasma sprayed deposits can result in a uniform distribution of the reinforcement throughout the $MoSi_2$ matrix and can enhance the matrix/reinforcement bonding. A review of $MoSi_2$-based composites which has been produced at the thermal spray facility at Los Alamos National Laboratory (LANL) will be discussed in this manuscript. Results will be presented on ductile phase toughened, laminate, and reactive plasma sprayed $MoSi_2$ composites in addition to $MoSi_2$ composites which were produced from composite powders which have been manufactured by a high temperature combustion synthesis process.

Ductile Phase Toughened $MoSi_2$ -Ta Composites

To improve the room temperature fracture toughness of polycrystalline $MoSi_2$, which is typically 3.0 MPa $m^{1/2}$, a ductile reinforced composite of $MoSi_2$ containing 10 and 20 vol% of a discontinuous tantalum reinforcement was produced by vacuum plasma spraying a mechanical blend of $MoSi_2$ and tantalum powders, Fig. 1a. The room temperature fracture toughness, K_{IC}, of these composites

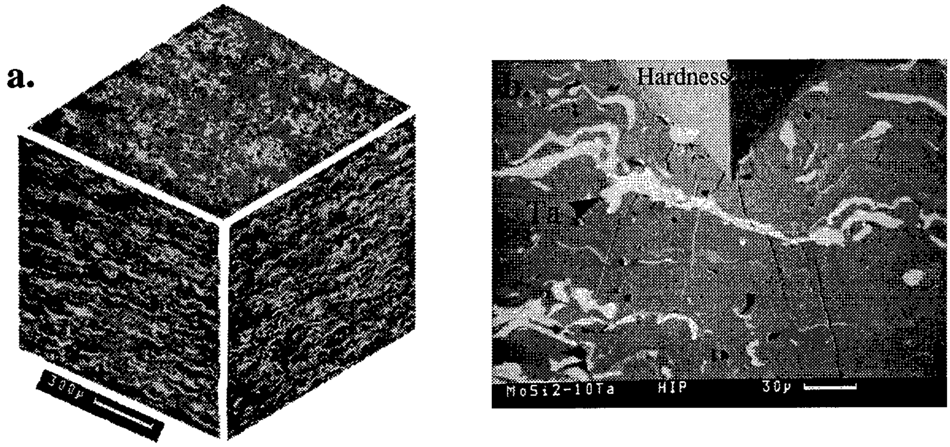

Fig. 1. a) 3-dimension view of a plasma sprayed ductile reinforced composite of $MoSi_2$ containing 20 vol. % tantalum, b) cracks propagating from a hardness indent in a $MoSi_2$-Ta composite demonstrating crack bridging, crack deflection and crack blunting.

was investigated using both an indentation fracture toughness test and a chevron notched four-point bend test (2). Samples were tested in the as-deposited condition and after hot isostatic pressing at 1200 °C at 206 MPa for 1 hour. A 50% increase in the room temperature fracture toughness was observed (from 3.0 to 4.5 MPa $m^{1/2}$) for unreinforced plasma sprayed $MoSi_2$. A substantial increase in the room temperature fracture toughness was observed with the additions of the ductile Ta phase resulting in K_{IC} values on the order of 10 MPa $m^{1/2}$. The toughness and mechanisms of toughness enhancement of the $MoSi_2$-Ta composites were evaluated using *in situ* fracture monitoring (13). Crack bridging, crack deflection and crack blunting, Fig.1b, was observed in the $MoSi_2$-Ta composites resulting in an R-curve behavior, Fig. 2.

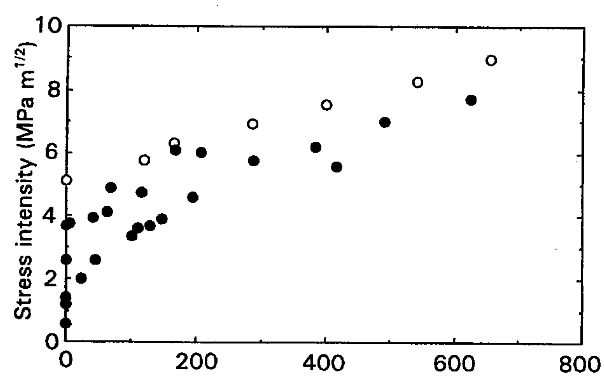

Fig. 2. Stress intensity (K) versus crack extension (Δa) plot constructed from *in situ* fracture observations. (•) cracks advancing normal to the surface of individual splats, (◦) cracks advancing parallel to surface of individual splats.

The orientation of an advancing crack with respect to the plasma sprayed microstructure affected the initiation and peak toughness of the samples tested. Cracks which propagated perpendicular to the surface of the individual splats which makeup the bulk of the composite (i.e., in the sprayed direction) had an initiation fracture toughness of 3 MPa $m^{1/2}$. Cracks which propagated parallel to the surface of the individual splat layers (i.e., normal to the spray direction) had an initiation fracture toughness of 5 MPa $m^{1/2}$. As the crack extended to 700 μm the fracture toughness increased to approximately 9 MPa $m^{1/2}$. Results reported by Castro *et al.* (2) for indentation and chevron notch 4-point bend tests showed good agreement with the *in situ* results.

Laminate Composites of $MoSi_2$-Al_2O_3

To improve the high temperature strength and damage tolerance of $MoSi_2$ above its ductile transition temperature (~1000°C) laminate composites of $MoSi_2$-Al_2O_3 were fabricated by plasma spraying alternate layers of $MoSi_2$ and Al_2O_3. Historically, improvements in the high temperature strength of $MoSi_2$ have been produced by the additions of discontinuous reinforcements in the form of particulates, platelets and whiskers of Si_3N_4, SiC, TiB_2, ZrO_2 and Al_2O_3 (10-12). The high temperature deformation and damage accumulation of laminate composites produced by plasma spraying were investigated by Bartlett and Castro (14). Results from high temperature mechanical testing showed that stable crack advancement could occur without catastrophic failure as long as the ductile $MoSi_2$ layers were sufficiently thick to temporarily stabilize the crack against further advancement. Mechanisms for crack propagation in the $MoSi_2$-Al_2O_3 composite were as follows: The cracks initiated in the Al_2O_3 at some stochastically determined stress level. A dominate crack could subsequently advance into the next Al_2O_3 layer if the stress intensity at the tip of the crack was above some critical value which would allow propagation through the ductile $MoSi_2$ layer. Thin layers of $MoSi_2$ resulted in catastrophic advancement of a crack due to a lower critical stress intensity. As the thickness of the $MoSi_2$ layers increased, multiple cracking occurred in the Al_2O_3 layers. Four-point bend testing results at 1200°C of different volume fractions (thickness) of $MoSi_2$ have shown an increase in yield strength, modulus and ultimate strength with volume fractions of 67% and 50% over monolithic $MoSi_2$, Fig. 3.

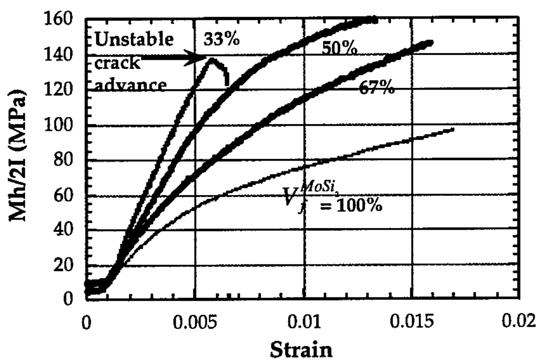

Fig. 3 M-e curves for plasma sprayed $MoSi_2$-Al_2O_3 composites tested at 1200°C with a cross-head speed of 0.4 μm/sec (14).

With the exception of 33 v/o of $MoSi_2$ all tests were terminated prior to failure. As indicated by the total area under the M-e curves, work of fracture increased with an increase in the volume fraction of $MoSi_2$. The ductile $MoSi_2$ layers at 1200 °C act as bridging ligaments shielding the crack tip and preventing catastrophic failure. The transition from multiple cracking to advance of a single catastrophic crack is dependent upon the relative thickness of the $MoSi_2$ layers. A critical thickness exists at which the bridging $MoSi_2$ ligament exerts sufficient tractions to allow for multiple cracking in the crack wake to occur in preference to a dominate crack advancing into the next Al_2O_3 layer. Debonding is not a requirement for multiple cracking. Constrained yielding and crack interactions are also proposed as mechanisms to further stabilize crack growth. Large strains to failure and associated high work of fracture are possible in the plasma sprayed laminate geometry. Figure 4 illustrates a $MoSi_2$-Al_2O_3 laminate composite 4-point bend test beam (2.54 cm long x 2mm wide x 2 mm thick) which was tested at 1400 °C. Interface debonding, plastic deformation of the silicide and multiple cracking all contribute to energy absorbing mechanisms observed in the composite beam. Deformation mechanisms depend upon yield strength of the deforming phase, interface fracture energy, relative volume fractions, strain rate, and testing temperature.

$MoSi_2$-Al_2O_3 laminate gas injection tubes have been plasma spray-formed and immersion tested at Air Products and Chemicals, Inc., in two different melts: Cu and Al-5 wt. %Mg (15). Results of the test showed that the composite tubes had substantial resistance to thermal shocking upon immersion into the molten metals. The composite tubes outperformed high-grade graphite and SiC tubes when immersed in molten copper and had similar performance to high density graphite and mullite when immersed in molten aluminum. Energy absorbing mechanisms such as debonding between the $MoSi_2$ and Al_2O_3 layers and microcracking in the Al_2O_3 layer contributed to the ability to absorb thermal stresses and strain energy during the performance test.

$MoSi_2$-Si_3N_4 Plasma Sprayed Composites Produce from Composite Powders

Plasma sprayed composites of $MoSi_2$-Si_3N_4 were produced from composite powders which were manufactured by Exotherm Corporation (1035 Line St.

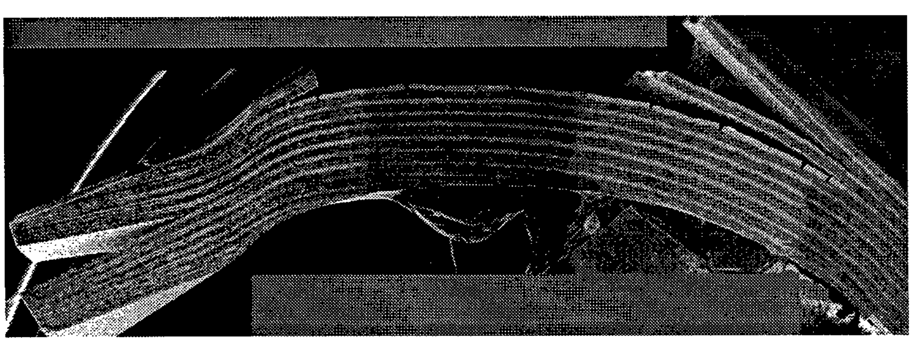

Figure 4. Four point bend test beam after testing at 1400°C. Extensive debonding at the $MoSi_2$/Al_2O_3 interface and cracking within the Al_2O_3 was observed.

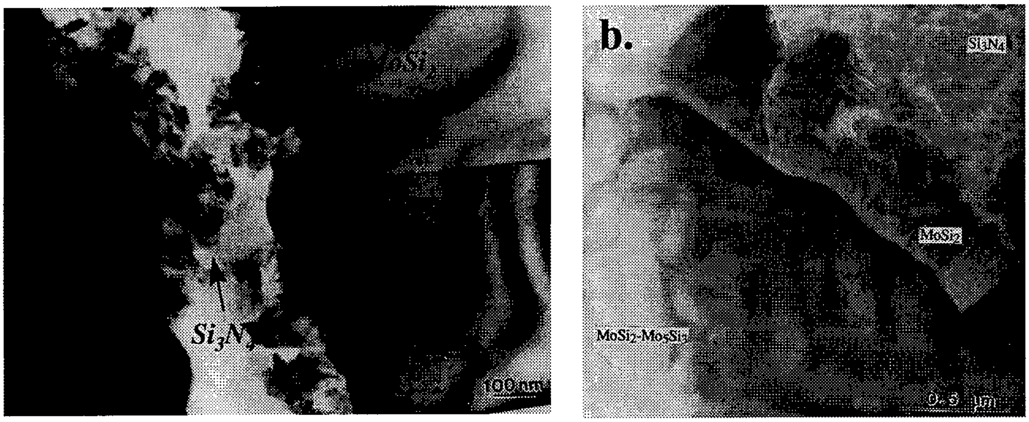

Fig. 5. a) TEM of SHS composite powders of $MoSi_2$-Si_3N_4, b) TEM of plasma sprayed $MoSi_2$-Si_3N_4 composite [16].

Camden, N.J. 08103) using a self-propagating high temperature synthesis (SHS) technique. Powders which are produced by the SHS process can incorporate submicron size reinforcements into the source powder which can be subsequently captured in the plasma sprayed deposit. The objective of this investigation was to evaluate whether the $MoSi_2$ matrix powders would shield the Si_3N_4 reinforcement from subliming during the plasma spray process in order to increase the volume fraction of Si_3N_4 in the $MoSi_2$ matrix. The starting powders produced by the SHS process contained a matrix of $MoSi_2$ with 75 nm reinforcements of β-Si_3N_4, Fig. 5a. The plasma sprayed deposits produced from this starting powder had both α and β Si_3N_4 reinforcements with a grain size of 150 nm. $C11_b$ -$MoSi_2$ with a large volume fraction of C40-$MoSi_2$ was the matrix material present in the deposit. A large volume fraction of Mo_5Si_3 was also identified, Fig. 5b. The Si_3N_4 reinforcements were agglomerated along the outside edges of the $MoSi_2$ particles as seen in Fig. 5a. Si_3N_4 enclosed by $MoSi_2$ is a more desirable arrangement since during the spray process the molten $MoSi_2$ would provide a protective shell around the Si_3N_4 to prevent it from sublimation. TEM and x-ray diffraction results revealed that a small fraction of the Si_3N_4 (less than 5 wt.%) was retained during plasma spraying of the SHS powders. This low value was a result of the sublimation of Si_3N_4 during the deposition process. The Si_3N_4 reinforcements, which were enclosed by $MoSi_2$ grains, were nonuniformily distributed throughout the plasma sprayed deposit, Fig. 5b. A detailed description of the structural characterization of combustion synthesized $MoSi_2$-Si_3N_4 composite powders and plasma sprayed $MoSi_2$-Si_3N_4 composites is given in reference (16).

Thick plasma sprayed deposits were produced using the $MoSi_2$-Si_3N_4 SHS composite powder. The flexure strength of the deposits were evaluated using 4-point bend testing at 1200 °C, at a strain rate of 10^{-5}/sec, Fig. 6.

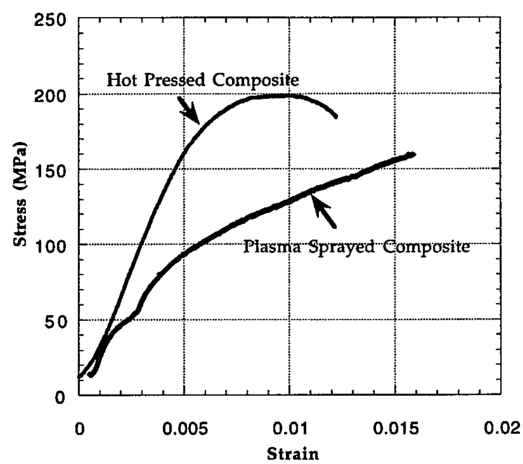

Fig. 6. Comparison of the stress-strain response of plasma-sprayed $MoSi_2$-Si_3N_4 with hot pressed $MoSi_2$-Si_3N_4 tested at 1200 °C and 10^{-5}/sec. Both composites were made from SHS powders.

The plasma sprayed material showed lower yield strengths and ultimate strengths when compared to conventional hot pressed $MoSi_2$-Si_3N_4 SHS powders. The plasma sprayed deposits exhibited a power-law hardening behavior and a larger strain tolerance than the hot pressed material. The power law behavior indicates hardening without significant damage development. A substantial amount of Mo_5Si_3 was found within the plasma sprayed deposits. Image analysis of the deposits revealed 25-30% Mo_5Si_3 present within the deposit. Because Mo_5Si_3 is lineraly-elastic at 1200 °C (17) the increase in mechanical properties of the sprayed SHS powders can be attributed to the trisilicide acting as a reinforcing phase. A detailed description of the mechanical testing results is discussed in reference (18). Impression creep investigations have also been performed on air plasma sprayed $MoSi_2$-Si_3N_4 composites (19). In general, a number of factors can affect the creep behavior of these composites including the degree and type of porosity, the fine grain size (1 to 10 µm) and the weak inter-splat bonds which can separate during impression creep testing.

Reactive Plasma Sprayed $MoSi_2$-SiC Composites

Plasma spraying of $MoSi_2$ using a Ar-10%CH_4 (methane) powder carrier gas mixture was investigated as a way of incorporating carbon and carbide particles into spray deposits of $MoSi_2$ which could subsequently getter SiO_2 after elevated temperature exposure (6). The presence of SiO_2 along grain boundaries in $MoSi_2$ can result in grain boundary sliding at elevated temperatures reducing the high temperature properties $MoSi_2$. TEM and parallel energy loss spectroscopy (PEELS) identified the presence of amorphous carbon particles along splat boundary regions in as-sprayed $MoSi_2$ when using the Ar-10%CH_4 powder gas mixture, Fig. 7.

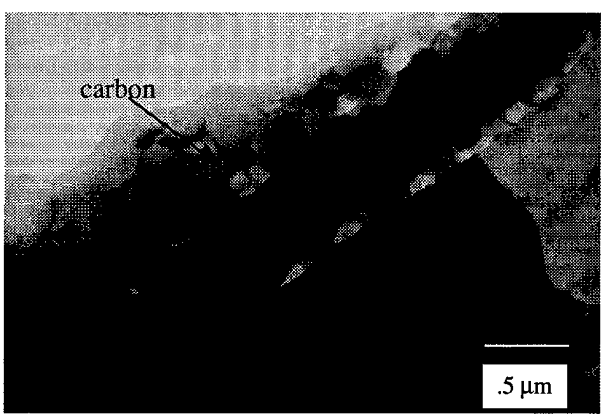

Fig. 7. Amorphous carbon particles along splat boundaries in as-sprayed $MoSi_2$ when using an Ar-10%CH_4 powder carrier gas mixture (6).

In addition to carbon particles, both α-SiC and β-SiC particles were also identified along inter-splat regions of the plasma sprayed deposit. The formation of SiC was a result of in-flight reactions which occurred between $MoSi_2$ particles and the reactive CH_4 powder carrier gas. Chemical analysis of the spray deposits revealed an increase in the carbon content from 750 ppm to 8380 ppm when spraying with the Ar-10%CH_4. A decrease in oxygen, from 2580 ppm to 750 ppm, was also observed after hot isostatic pressing the plasma sprayed samples at 1800 °C and 206 MPa for 1 hour, Table 1.

Table 1. Carbon and oxygen analysis of $MoSi_2$ feedstock powder and plasma sprayed deposits.

Material	Carbon (wt.%)	Oxygen (wt.%)
as-received $MoSi_2$	0.0516 + 0.0004	0.161 + 0.0003
as-sprayed $MoSi_2$	0.0749 + 0.0063	0.146 + 0.007
as-sprayed $MoSi_2$-CH_4	0.838 + 0.035	0.258 + 0.013
$MoSi_2$ (HIPed)	0.105 + 0.017	0.164 + 0.014
$MoSi_2$-CH_4 (HIPed)	0.420 + 0.062	0.075 + 0.019

Deposits produced using the Ar-10%CH_4 powder gas mixture and HIPed at 1800 °C and 206 MPa for 1 hour exhibited a factor of three increase in yield strength over conventional hot pressed $MoSi_2$ when tested in four-point bending at temperatures between 1100°C and 1400°C, Fig. 8.

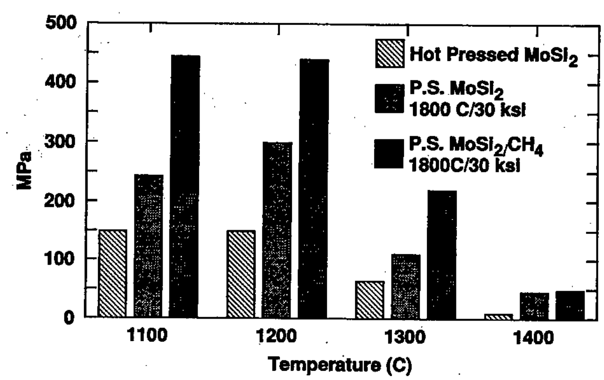

Figure 8. Yield strength in 4-point bending as a function of temperature for hot-pressed and plasma sprayed $MoSi_2$ with and without the use of an Ar-CH_4 powder carrier gas.

The increase in yield strength was attributed to a decrease in SiO_2 along the grain boundaries in the $MoSi_2$ matrix minimizing grain boundary sliding at the elevated test temperatures. Increases in the yield strength of $MoSi_2$ sprayed without the Ar-CH_4 powder gas mixture was attributed to a dispersion strengthening effect which resulted from a fine distribution of Mo_5Si_3 precipitates in the spray deposits. Precipitates of Mo_5Si_3 resulted from a loss of Si during the high temperature plasma spray process. Fuel burner nozzles for high temperature burner applications have been produced by reactive plasma spraying $MoSi_2$ on a converging/diverging graphite mandrel which is subsequently oxidized out after spraying to provide a free-standing net-shape nozzle, Fig. 9.

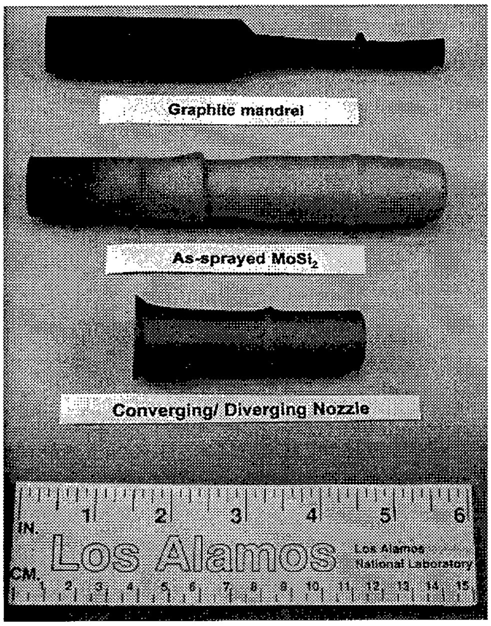

Fig. 9. Fuel burner nozzle produced by reactive plasma spraying $MoSi_2$.

Summary

Plasma spraying of $MoSi_2$ composites with secondary reinforcements of Ta, Al_2O_3, Si_3N_4, SiC and Mo_5Si_3 has been demonstrated. The introduction of a secondary reinforcing phase can result in an improvement in the low temperature fracture toughness and high temperature strength of the $MoSi_2$ matrix. Plasma spraying offers the flexibility to produce continuous and discontinuous reinforced composites of $MoSi_2$-based materials with tailored microstructures. Application of this technology includes high temperature oxidation resistant coatings and structural components.

References

1. Tiwari, R., H. Herman, and S. Sampath, S., Mater. Sci. Eng., Vol A155, 95-100 (1992).
2. Castro, R.G., R.W. Smith, A.D. Rollett, and P.W. Stanek, Mater. Sci. Eng., Vol A155, 101-107 (1992).
3. Alman, D.E., K.G. Shaw, N.S. Stoloff and K. Rajan, Mater. Sci. Eng., Vol A155, 85-93 (1992).
4. Smith, R.W., , Powder Metall. Int., Vol 25, 9-16 (1993).
5. Sampath, S., and H. Herman, Mat. Res. Soc. Sympo. Proc. Vol. 322. 71-82 (1994).
6. Castro, R.G., H. Kung and P.W. Stanek, Mater. Sci.Eng., Vol. A185, 65-70 (1994).
7. Castro, R.G., , J.R. Hellmann, A.E. Segall and D.L. Shelleman, Mater. Res. Soc. Symp. Proc., Vol 322, 81-87 (1994).
8. Jeng, Y.L., and E.J. Lavernia, J. Mater. Sci., Vol 29, 2557-2571 (1994).
9. Ling, X., E.J. Lavernia, J. Wolfenstine and A. Sickinger, J. of Thermal Spray Technology, 4(3) 252-260, (1995).
10. Vasudevan, A.K., and J.J. Petrovic, Mater. Sci. Eng., A155, 1 (1992).
11. Petrovic, J.J., MRS Bull. XVIII 35, (1993).
12. Petrovic, J.J., and A.K. Vasudevan, Mater. Res. Soc. Symp. Proc., 322, 3 (1994).
13. Rigney, J.D., R.G. Castro and J.J. Lewandowksi, J. of Mat. Sci. 28, 4023-4027 (1993).
14. Bartlett, A.H., and R.G. Castro, accepted for publication in Acta Metall. Mater., (1997).
15. Bartlett, A.H. R.G. Castro, D.P. Butt, H. Kung, Z. Zurecki and J.J. Petrovic, Industrial Heating, January 33-36 (1996).
16. Kung, H., Y.C. Lu, A.H. Bartlett, R.G. Castro and J.J. Petrovic, accepted for publication in J. of Mat. Res. (1997).
17. Gibala, R., H. Chang, and C.M. Czarnik, Mat. Res. Soc. Symp. Proc., 322, 175-183 (1994).
18. Bartlett, A.H., and R.G. Castro, accepted for publication in the Journal of Material Science (1997).
19. Hollis,K.J., D.P. Butt and R.G. Castro, United Thermal Spray Conference Proceedings, September 15-18, Indianapolis Id, (1997).

M98001610

Report Number (14) LA-UR--97-3721
CONF-980533--

Publ. Date (11) 19980525
Sponsor Code (18) DOE/EE, XF
UC Category (19) UC-1425, DOE/ER

DOE